# First-Principles Study of Ethylene on Ge(001)—Electronic Structures and STM Images

**X. L. Fan,*,† Q. Cheng,† Q. Chi,† Y. F. Zhang,‡ and W. M. Lau§**

*School of Material Science and Engineering, Northwestern Polytechnical University, 127 YouYi Road West, Xian, 710072, Shaanxi, China, Department of Chemistry, Fuzhou University, Fuzhou 35002, China, and Surface Science Western, University of Western Ontario, London, Ontario, N6A 5B7, Canada*

*Received: February 9, 2010; Revised Manuscript Received: July 23, 2010*

By using the first-principles density functional theory, we calculate the partial charge densities and STM images for the intradimer di-$\sigma$ and interdimer end-bridge adsorption configurations of ethylene on Ge(001). Our simulated STM images show the effects of ethylene adsorption and clarify that, although STM images and surface structures evolve as the adsorption sites of ethylene on Ge(001), the molecular orbitals of the bare Ge atoms always remain the dominating electronic states near the Fermi level. For the di-$\sigma$ model, the display of such dominance in STM images is, however, damped by the preferred tunneling paths between the tip and the electronic states of ethylene due to their short tunneling distances. In comparison, the distance between the tip and the end-bridge bound $C_2H_4$ molecules is not so short relative to the distance between the tip and the up-Ge atoms of the bare Ge—Ge dimer; hence, the dominance of bare up-Ge atoms can still be found in the STM images at low bias voltages. Our simulated STM results confirm that the di-$\sigma$ and paired-end-bridge configurations are observable adsorption structures for $C_2H_4$ on Ge(001). The comparisons of the STM images between Ge(001) and Si(001) reveal the distinction of their highest occupied surface states, which explains the differences in geometry and reactivity of adsorbates, including $C_2H_4$ and $O_2$, on Ge(001) versus Si(001).

## 1. Introduction

The adsorption of unsaturated hydrocarbon molecules on the Si(001) and Ge(001) surface has attracted great interest because of its potential in technological applications, such as nonlinear optical devices, chemical sensors, and molecular electronic devices.[1] Ge(001) and Si(001) surfaces have similar atomic structures; particularly, both of these surfaces undergo reconstruction to form dimers. The electronic structure of both surfaces are also alike.[2−5] Therefore, the adsorption structures of unsaturated hydrocarbons on Si(001) and Ge(001) are expected to be similar with each other. However, there are some intrinsic features of these two surfaces that sometimes result in them exhibiting quite different physical and chemical behaviors,[6] such as different geometries and reactivities, of molecules on the Ge surface[7,8] compared with the Si surface. Such features have attracted substantial attention very recently.[9−11]

Ethylene, $C_2H_4$, is one of the most studied unsaturated hydrocarbons on Si(001) and Ge(001). There are two possible binding models for $C_2H_4$ adsorption on both Si(001) and Ge(001), as shown in Figure 1: (a) intradimer di-$\sigma$ model in which an $C_2H_4$ molecule adsorbs on top of a single dimer by forming two $\sigma$ bonds between C and Si(Ge) atoms and (b) interdimer end-bridge model in which an $C_2H_4$ molecule bridges upon one atom of a dimer and a neighboring atom of an adjacent dimer.

A variety of experimental studies, such as scanning tunneling microscopy (STM),[1,12] near-edge X-ray adsorption fine structure (NEXAFS),[13,14] angle-resolved photoemission spectroscopy (ARPES),[15] photoelectron diffraction imaging,[16] and reflectance anisotropy spectroscopy,[17] have concluded that $C_2H_4$ chemisorbs on top of a single Si dimer by forming the di-$\sigma$ structure from low to high coverage. Many theoretical ab initio calculations have been performed in the recent years,[17−19] and all calculations agree that the intradimer di-$\sigma$ configuration is more energetically favorable than the interdimer end-bridge configuration at a coverage of 0.5 ML, whereas the paired-end-bridge configuration is more energetically favorable than the paired-di-$\sigma$ configuration at a coverage of 1.0 ML. Using a slab model, Cho and Kleinman[18] identified the addition barriers for $C_2H_4$ to form the di-$\sigma$ and end-bridge structures, which are 0.02 and 0.12 eV, respectively. To further examine the adsorption details, we have recently studied $C_2H_4$ adsorption on both Si(001) and Ge(001) by calculating ab initio molecular dynamics (AIMD) as well as potential energy surfaces for possible reaction channels, as a function of $C_2H_4$ coverage.[19,20] Similar to the results of Cho and Kleinman, our findings[19] also showed that, on Si(001), the formation of the di-$\sigma$ structure is easier than the end-bridge structure by a difference of 0.1 eV in energy barrier, whereas the reaction barrier for the adsorption of the second di-$\sigma$ $C_2H_4$ is the same as that for the second end-bridge

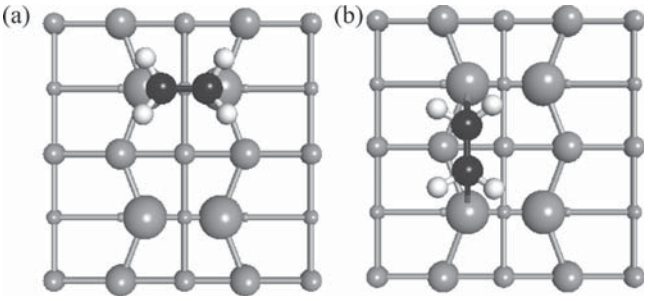


**Figure 1.** Possible binding models of $C_2H_4$ adsorption on the Ge(Si)(001) surface: (a) di-$\sigma$ model and (b) end-bridge model.

* To whom correspondence should be addressed. E-mail: xlfan@nwpu.edu.cn.
† Northwestern Polytechnical University.
‡ Fuzhou University.
§ University of Western Ontario.

10.1021/jp101275j 
Published on Web 08/11/2010

$C_2H_4$. In addition, our study also examined one more adsorption configuration involving the sublayer Si atoms and concluded that the formation of this configuration is unlikely for $C_2H_4$ but is important in the case of $C_2H_2$ adsorption.

The case of $C_2H_4$ on Ge(001) is far more controversial than that of $C_2H_4$ on Si(001). For example, Bent and co-workers suggested the existence of two adsorption states, which is supported by their temperature-programmed desorption (TPD) measurements of two desorption features at almost all coverages.[21] Later, Fink et al., however, concluded the presence of only one chemisorbed structure, namely, the di-$\sigma$ structure, with their results from TPD and angle-resolved photoemission (ARUPS).[22] A more recent study by Kim et al. showed[23] two desorption features with desorption energies of 1.05 and 1.15 eV, with TPD and scanning tunneling microscopy (STM) as their analysis tools. These respective features were assigned as the di-$\sigma$ and paired-end-bridge configurations, in accord to their observed STM features. Not unlike the variations in the reported experimental data, the computational study of $C_2H_4$ on Ge(001) has also not been straightforward. The earliest first-principles report[24] confirmed the existence of the di-$\sigma$ configuration but ruled out the end-bridge structure. In addition, the report also speculated that the end-bridge structure is metallic. In our recent re-examination of this adsorption system with ab initio total energy and reaction pathway analysis,[20] we showed that both di-$\sigma$ and end-bridge configurations can be formed on the Ge(001) surface with coverages at 0.5 and 1.0 ML. Furthermore, we also clarified the mixed-mode adsorption cases with the following conclusions: (a) first, $C_2H_4$ being adsorbed with the end-bridge configuration and, second, $C_2H_4$ being adsorbed with the di-$\sigma$ configuration and (b) first, $C_2H_4$ with the di-$\sigma$ configuration and, second, $C_2H_4$ with the end-bridge configuration. Energetically, the two mixed-mode adsorption cases are less favorable than the single-mode adsorption cases (pure di-$\sigma$ and pure end-bridge). In short, we concluded that the di-$\sigma$ and paired-end-bridge configurations are more favorable for $C_2H_4$ adsorption on Ge(001).

In the present study, building upon the optimized structures obtained by the total energy calculations, we have further calculated the partial charge densities and simulated the STM images for the bare surface and the adsorbed surfaces of the di-$\sigma$ and end-bridge configuration, plus the paired-di-$\sigma$ and paired-end-bridge configurations. For these calculations, we have adopted the Tersoff−Hamann theory.[25] Moreover, to demonstrate the different adsorptions between $C_2H_4$ on Si(001) and on Ge(001), we have further studied the possible adsorption involving the sublayer atoms, in addition to comparing the STM images of Ge(001) with those of Si(001). These results are important as they explain the STM experiments and prove two adsorption configurations of $C_2H_4$ on Ge(001). The results in this present study also clearly display the different highest occupied surface states on Si(001) in reference to those on Ge(001). The comparison explains the differences in geometry and reactivity of adsorbates on the Ge surface versus the Si surface.

## 2. Calculation Methods

The geometry optimization and electronic structure calculations in the present study were performed on the basis of density functional theory with the Vienna ab initio simulation package (VASP).[26−29] The reported calculations have been carried out using the Vanderbilt ultrasoft pseudopotential[30−32] and plane-wave method. The generalized gradient approximation (GGA)[33] of Perdew−Wang (PW91) has been used for calculating the electronic exchange-correlation potential.

The calculations were performed using the p(2 × 2) and the c(4 × 2) reconstructed Ge(001) surfaces, which are the two most stable reconstructed structures. Both were simulated by a slab containing eight Ge atomic layers and a vacuum region with a spacing of 12.94 Å, while the dangling bond of the bottom Ge atoms were terminated by H atoms. The bulk lattice constant was determined to be 5.75 Å. The structure optimizations were performed using the calculated bulk lattice constant. The terminating hydrogen atoms and the Ge atoms in the bottom layer of the slab were fixed to the bulk position. In the total energy calculations, the Brillouin zone was sampled by a Monkhorst−Pack scheme with 4 × 4 × 1 and 2 × 2 × 1 $k$-point grids for the p(2 × 2) surface with a 2 × 2 cell and the c(4 × 2) surface with a 4 × 4 cell, respectively. The STM images were simulated using the Tersoff−Hamann formula and its extension.[25] Briefly, assuming that the density of states of the tip is constant and the STM imaging is conducted by maintaining the tip at a constant height with a relatively small tunneling current, we can approximate the STM tunneling current with the following expression with the local density of states, $\rho(\vec{r}, E)$, as the only variable

$$I(V) \propto \int_{E_F}^{E_F+eV} \rho(\vec{r}, E)\mathrm{d}E$$

$$\rho(\vec{r}, E) = \sum_i |\psi_i(\vec{r})^2|\delta(E - E_i)$$

where $\rho(\vec{r}, E)$ is the LDOS on the sample surface, $\psi_i(\vec{r})$ is the sample wave function with energy $E_i$, and $E_F$ is the Fermi energy. When the states in $\rho(\vec{r}, E)$ are filled, it is also common to refer to $\rho(\vec{r}, E)$ as the charge density of the states. In the present work, the LDOS are also expressed in the Cartesian coordinates $\rho(x,y,z,E)$ with $z$ as the vertical direction and $z = 0$ at the position of the adsorbed surface dimer. To further clarify the STM contrast contributions from the various groups of LDOS that are derived from the main surface constituents, such as the up-Ge, the back-bond, and the H and C atoms of the $C_2H_4$ molecule, we have also calculated and plotted the $z$-line-profiles of such LDOS groups. As expected, the $z$-line profiles are particularly relevant to the STM imaging contrast because $\rho(x,y,d,E)$, when $d$ is the location of the STM tip, is proportional to the STM contrast. Hence, comparing the $\rho(x,y,z,E)$ of the main surface constituents in $z$-line profiles at the proximity of the possible STM tip location can reveal the chemical bonding information encoded in an STM image.

## 3. Results and Discussion

**3.1. Sublayer Adsorption.** As discussed earlier, in addition to the intradimer di-$\sigma$ and interdimer end-bridge adsorption models on Ge(001), there is still another possible adsorption model: the adsorption between a sublayer Ge atom and a dimer Ge atom. Such a kind of adsorption has been studied for $C_2H_4$ and $C_2H_2$ on Si(001) in our recent report.[19] The adsorption leads to the formation of a "sub-di-$\sigma$" configuration. In the present work, the similar adsorption geometry has been studied for $C_2H_4$ on Ge(001). In brief, in the trials of finding a stable geometry for $C_2H_4$ adsorption between the sublayer Ge atom and a dimer Ge atom by structure optimizations, the adsorption on the sublayer Ge atom turns out to be endothermic; the adsorption energy is about −0.2 eV. Hence, the presence of "sub-di-$\sigma$" adsorption is unlikely.

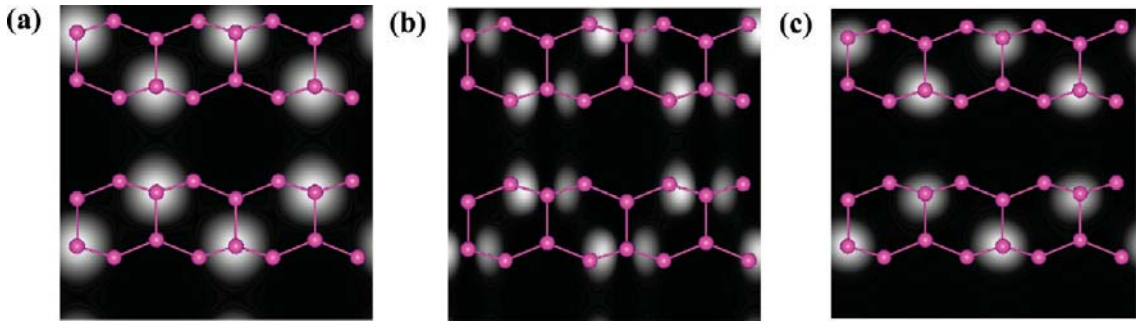


**Figure 2.** Simulated STM images of the bare Ge(001)c(4 × 2) surface with (a) $V_S = -0.5$ V, (b) $V_S = -0.1$ V, and (c) $V_S = -0.3$ V.

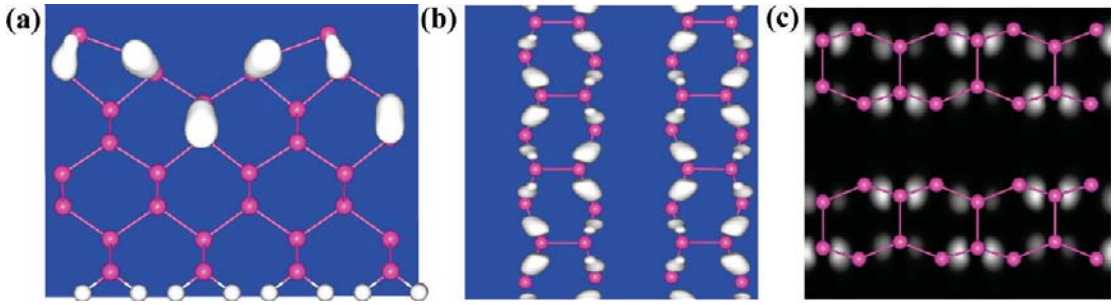


**Figure 3.** Partial charge density for the bare Ge(001)c(4 × 2) surface with $V_S = -0.1$ V (isosurface value = $1.5 \times 10^{-3}$ e/Å$^3$): (a) side view and (b) top view. (c) Simulated STM image of the bare Ge(001)c(4 × 2) surface with $V_S = -0.1$ V with the tip set just above the surface.

**3.2. Simulated STM Images.** With the sub-di-$\sigma$ adsorption being ruled out for $C_2H_4$ on Ge(001), together with the previous conclusion of the absence of any mixed-mode adsorption,[20] only the adsorption configurations of di-$\sigma$ and end-bridge, plus those of paired-di-$\sigma$ and paired-end-bridge are needed to be considered. Using the Tersoff−Hamann approximation, we have then simulated the STM images of these configurations. In addition, the STM images of the bare Ge(001) surface have also been computed as benchmark references for the $C_2H_4$ adsorbed surfaces. The basic features of the bare and adsorbed surfaces calculated with the p(2 × 2) and c(4 × 2) reconstructed surface are similar. Considering the fact that the c(4 × 2) reconstructed geometry is evident in the experimental STM for the bare Ge(001) surface,[34] the results calculated by the c(4 × 2) surface with a 4 × 4 cell are used in our following analysis.

***3.2.1. Simulated STM Images for the Bare Ge(001)c(4 × 2) Surface.*** The STM images of the Ge(001)c(4 × 2) surface with $V_S = -0.5$, $-1.0$, and $-1.5$ V are similar with each other, all displaying the bright spots on top of the up-Ge atoms, as shown in Figure 2a. These bright protrusions denote the high charge densities centered on the up-Ge atom of the dimer, which are derived from the dangling bond of the up-Ge atom formed from its $p_z$ orbital. When the integrated region decreases to $-0.1$ V, the pattern of the image in Figure 2b is the double-lobes located on both sides of the up-Ge atom, which is the characteristic of the back-bond states. The image with $V_S = -0.3$ V is shown in Figure 2c, which reveals the transition from the double-lobes shown in Figure 2b with $V_S = -0.1$ V to the round protrusions centered on the up-Ge atoms shown in Figure 2a with $V_S = -0.5$ V. This image also can be understood as the mixed feature of the back-bond and dangling bond surface states.

Our simulated images at a bias of $-0.5$ V agree well with the previous theoretical simulations of the STM images at high bias voltages, which denoted the high charge densities centered on the up-Ge atom for the Ge(001) surface.[34] The previous reported pattern of the image observed in the STM experiment under a high bias voltage is decorated by bright round spots on the up-Ge atom of the dimer, which is also shown by our computational results shown in Figure 2a. It is worth noting that there is a small difference between our simulation and the reported simulations at low bias voltages. The previous reported results showed that the pattern of the simulated image under a low bias voltage is the double-lobed pattern on the two sides of both the up- and the down-Ge atom of the buckled Ge−Ge dimer, with the pattern centered on the up-Ge atom much brighter than those on the down-Ge atom. In comparison, our simulated images in Figure 2b,c at low bias voltages show the double-lobed pattern only around the up-Ge atom. The partial charge density has been computed to further examine the cause of the inconsistency. As shown in Figure 3a,b, the partial charge density within 0.1 V below the $E_F$ clearly shows the features of the back-bond between the top layer and the second layer Ge atoms, where the back-bond surface states of the up-Ge atoms extend further into the vacuum region. In STM, commonly, the tip is set at around 3.0 Å above the top atom on the surface for simulating the STM image. If we decrease the height of the plane on which the STM image is scanning to just above the up-Ge atom, the pattern of the image with $V_S = -0.1$ V changes to what is shown in Figure 3c. The resulting STM image then looks like the previouly reported simulation, which displays the double lobes centered not only on the up-Ge atom but also on the down-Ge atoms with less brightness. Moreover, if one examines the experimentally observed image with $V_S = -0.1$ V in the reported results carefully, one finds that the STM image indeed looks like our simulation in Figure 2b generated with the tip−surface distance set at 3 Å.

***3.2.2. Simulated STM Images for the $C_2H_4$ Adsorbed Ge(001)c(4 × 2) Surface.*** In the vicinity of the Fermi level, the back-bond and dangling bond states of the surface Ge atoms, as well as the LDOSs of C and H atoms from the adsorbed $C_2H_4$ molecule, can all contribute to the STM images. In the process of simulating STM images, the line profiles of the partial charge density versus distance from the Ge(001) surface has been calculated as references and guidance to optimize the simulation. These lines are vertical through the H and C atoms

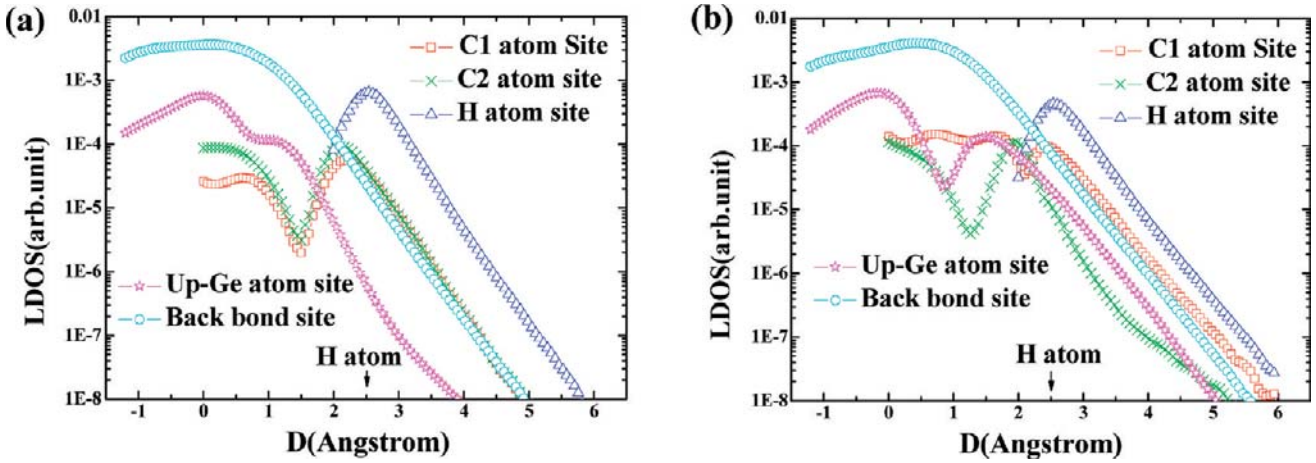


**Figure 4.** Vertical line profiles of calculated partial charge density versus distance from the Ge(001) surface for (a) the di-$\sigma$ structure with $V_S = -0.2$ V and (b) the paired-di-$\sigma$ structure with $V_S = -0.3$ V. Four curves representing the partial charge density on the vertical lines through C1, C2, H, and up-Ge atoms are shown. The arrow indicates the height of the top H atom of the $C_2H_4$ on Ge(001).

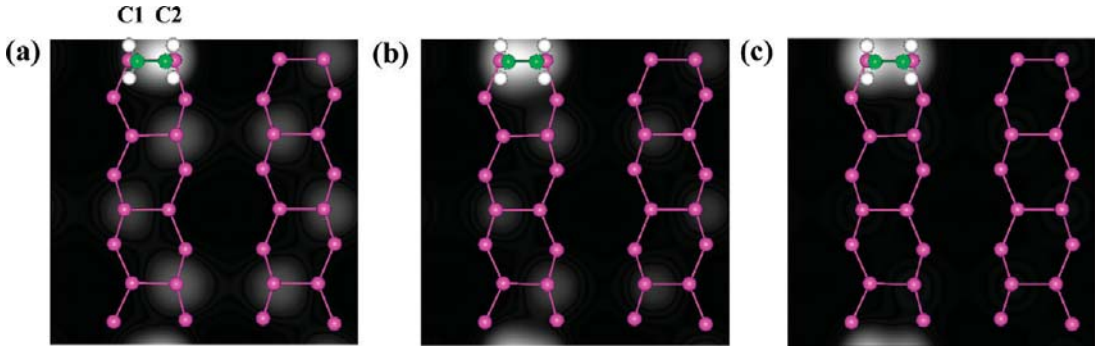


**Figure 5.** Simulated STM images of the di-$\sigma$ structure with (a) $V_S = -0.5$ V, (b) $V_S = -1.0$ V, and (c) $V_S = -1.5$ V.

of the $C_2H_4$ molecule, up-Ge atom of the unreacted dimer, which describes the contribution of the dangling bond states, and the center of the back bonds. In all of the line profiles shown in the present work, the zero point of the $z$ axis is set at the position of the adsorbed surface dimer and the minimum value at the position of the second layer Ge atom.

At a low bias voltage of $-0.2$ V, which is near the edge of the valence band at low coverage, as we have reported in our previous report,[20] only very few surface states are included in. As an example, the line profiles of the partial charge density for the di-$\sigma$ at $-0.2$ V are shown in Figure 4a. On the plane of 1 Å above the top H atom, the largest partial charge is only around $2 \times 10^{-5}$ e/A$^3$. In the case of high coverage, the band gap increases relative to the case of the low coverage. Accordingly, the partial charge density of the two paired structures has been calculated at $-0.3$ V. The line profiles of the paired-di-$\sigma$ configuration shown in Figure 4b show that the largest partial charge density on the plane of 1 Å above the top H atom is only around $3 \times 10^{-5}$ e/A$^3$. Hence, it is difficult to image the adsorbed surface effectively in the condition of without touching the adsorbed molecule at low bias voltages of $-0.2$ and $-0.3$ V. Actually, the range of sample biases used for effective imaging the $C_2H_4$ adsorbed Ge(001) surface in experimental STM is from $-1.0$ to $-1.8$ V.[23] Consequently, the lowest bias voltage to simulate STM images is set at $-0.5$ V in the present study.

Figure 5a−c shows the respective simulated images of filled states with $V_S = -0.5$, $-1.0$, and $-1.5$ V for the di-$\sigma$ configuration. The three images in Figure 5 are similar with each other; all of them show the protrusion centered on the $C_2H_4$ molecule, which is brighter than the protrusions on top of the up-Ge atom of the unreacted dimer (no $C_2H_4$ adsorption). The pattern of the protrusions on top of the $C_2H_4$ molecule is different from each other. At $-0.5$ V, the pattern is decorated by a bright round spot on top of the $C_2H_4$ molecule with the spot center at one of the two C atoms (C2). At $-1.0$ V, the pattern is decorated by a bright bean-shaped spot located between the two C atoms. At $-1.5$ V, the pattern is decorated by two connected bright round spots on top of the two C atoms. In addition, the bright contrast on top of the up-Ge atom decreases with the increase of the bias voltage.

For the paired-di-$\sigma$ structure with two di-$\sigma$ bound $C_2H_4$ molecules adsorbed on the two adjacent dimers, the STM images vary with the bias voltage similar to the di-$\sigma$ structure and the simulated STM images are similar to those of the di-$\sigma$ structure. If we replace the pattern of the bare up-Ge atom in the same dimer row and next to the adsorbed dimer with the pattern of the di-$\sigma$ adsorbed $C_2H_4$ molecule in Figure 5, we can get the STM images of the paired-di-$\sigma$ structure. All of the STM images show two parallel bright protrusions on the two adjacent dimers in the same dimer row and dimer protrusions on the up-Ge atoms of the bare dimer.

Our simulated STM images of filled states for the end-bridge structure under three bias voltage conditions ($V_S = -0.5$, $-1.0$, and $-1.5$ V) are shown in Figure 6a−c. As shown in Figure 6a, the image with $V_S = -0.5$ V shows a protrusion on the adsorbed $C_2H_4$ molecule centered on one of the two C atoms (C2) and a bright round spot on top of the unabsorbed up-Ge atoms. The spots on top of the bare up-Ge atoms near the adsorbed $C_2H_4$ molecule are brighter than those on top of the up-Ge atoms further away from the adsorbed molecule. That is because the adsorption on the end-bridge site changes the near

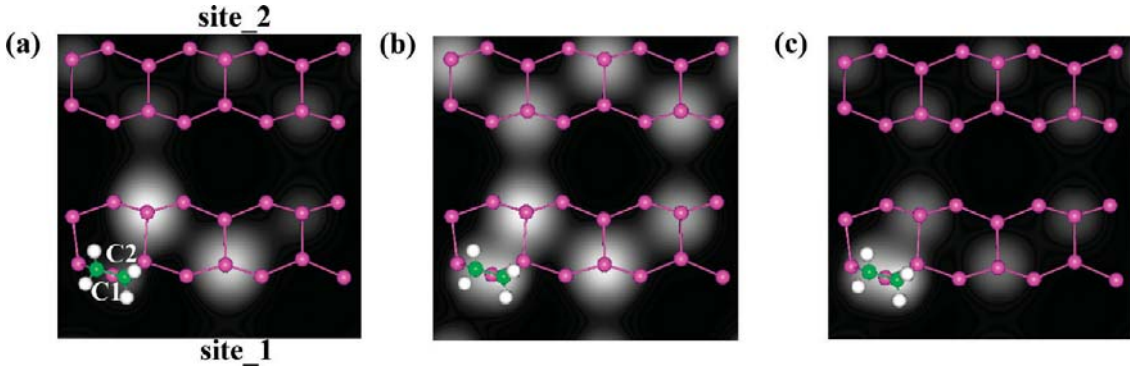


**Figure 6.** Simulated STM images of the end-bridge structure with (a) $V_S = -0.5$ V, (b) $V_S = -1.0$ V, and (c) $V_S = -1.5$ V.

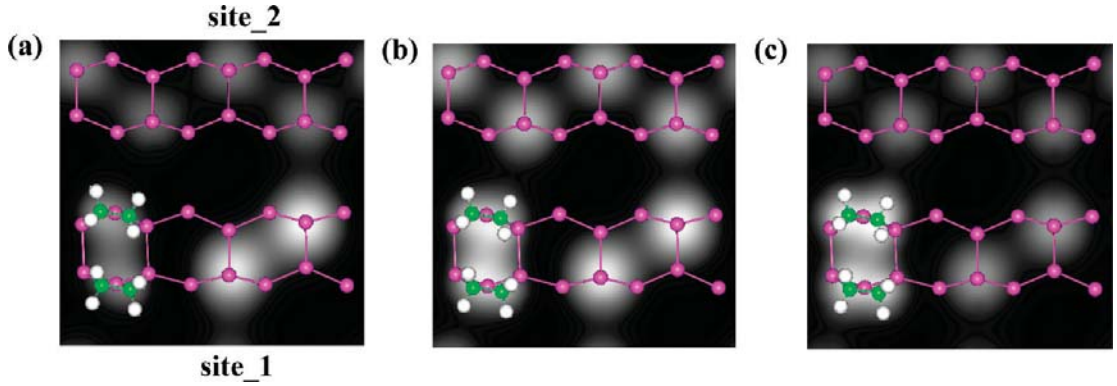


**Figure 7.** Simulated STM images of the paired-end-bridge structure with (a) $V_S = -0.5$ V, (b) $V_S = -1.0$ V, and (c) $V_S = -1.5$ V.

dimer and makes the $z$ coordinate of up-Ge a little higher. The corresponding electronic states will extend further into the vacuum, and thus, the images are brighter. The images with $V_S = -1.0$ and $-1.5$ V show the protrusion with a bean-shaped pattern on top of the $C_2H_4$ molecule and the protrusions on top of the up-Ge atoms, where the bright contrast on top of the up-Ge atom decreases at a bias of $-1.5$ V compared with those at a bias of $-1.0$ V.

For the paired-end-bridge configuration, the image with $V_S = -0.5$ V in Figure 7a shows the protrusions on the two adsorbed molecules centered around one of the two C atoms and protrusions on top of the unabsorbed up-Ge atoms. Again, the brightness of the pattern on top of the up-Ge atoms is distinctive, which can be explained by the difference of the $z$ coordinates between the up-Ge atoms near and further away from the adsorbed $C_2H_4$ molecule. The STM images with $V_S = -1.0$ and $-1.5$ V, as shown, respectively, in Figure 7b,c, display the pattern of two bright spots with one central node between two adjacent dimers in the same dimer row and the patterns of the dangling bond state centered on the unadsorbed up-Ge atoms.

As reported by Kim et al.,[23] there are two adsorption features on the $C_2H_4$ adsorbed Ge(001) surface. One is denoted as "Feature A", which is located on top of a dimer. The other one is denoted as "Feature B", which is located between two Ge−Ge dimers. The STM image of "Feature B" appears darker than that of "Feature A". This STM experiment is done at room temperature, and at such a condition, the bare Ge−Ge dimers are known to be symmetric. In the present work, the Ge(001) surface is modeled as a c(4 × 2) surface, which is the most stable reconstructed structure at low temperatures, and the corresponding Ge−Ge dimers appear as buckled with one Ge atom up and the other one down, as shown in the above simulated images for the bare dimers.

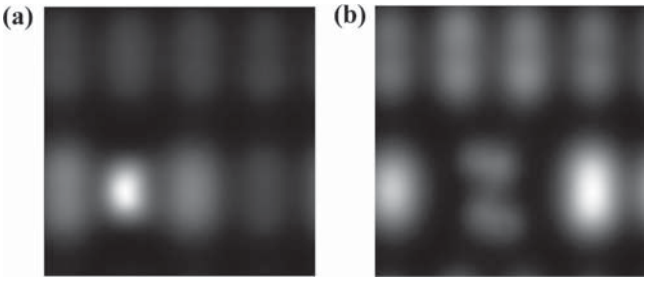


**Figure 8.** Simulated STM images: (a) the di-$\sigma$ structure on the Ge(001)(2 × 1) surface with $V_S = -0.8$ V and (b) the paired-end-bridge structure on the Ge(001)(2 × 1) surface with $V_S = -0.8$ V.

Among the above twelve images simulated for the four different adsorption configurations at different voltages, the images of the di-$\sigma$ structure with $V_S = -1.0$ V can be compared to the "Feature A" found in the STM experiment reported by Kim et al.,[23] which has protrusions located on top of a dimer and is brighter than the unreacted Ge dimer. In addition, our simulated images of the paired-end-bridge structure with $V_S = -1.0$ V have the same character as "Feature B" in this STM experiment.[23] As shown in Figure 7b, there are two local protrusions with one central node located on top of the two $C_2H_4$ molecules between two dimers. Furthermore, the bare Ge dimers in the di-$\sigma$ structure and the paired-end-bridge structure have been modified to model the symmetric dimer of the Ge(001)(2 × 1) surface observed at room temperature, and the STM images are computed. As shown in Figure 8a, the di-$\sigma$ adsorption appears brighter compared with the bare dimer. In comparison, the paired-end-bridge adsorption is imaged as darker than the bare Ge dimer, as shown in Figure 8b. Consequently, our calculated STM images for the di-$\sigma$ and paired-end-bridge structures agree well with the "Feature A" and "Feature B" adsorption observed in STM experiment.

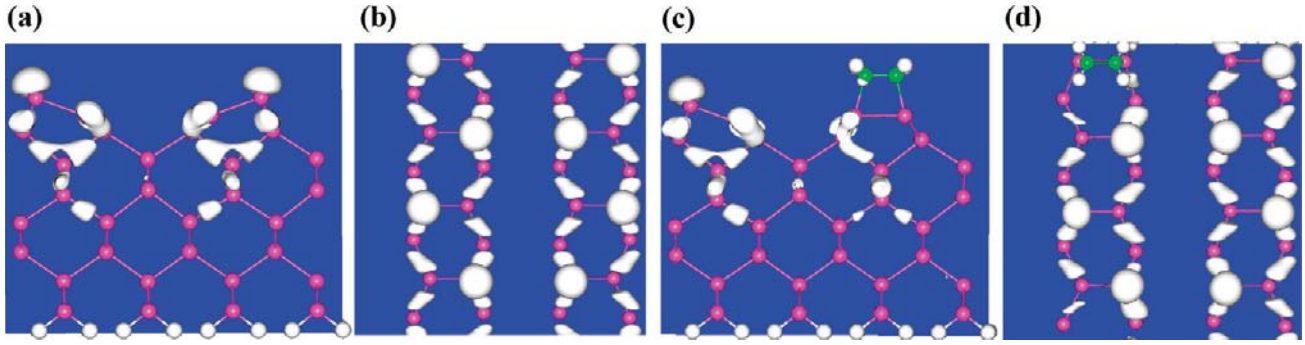


**Figure 9.** Partial charge density with $V_S = -0.5$ V for (a) the side view of the bare Ge(001)c(4 × 2) surface, (b) the top view of the bare Ge(001)c(4 × 2) surface, (c) the side view of the di-$\sigma$ structure, and (d) the top view of the di-$\sigma$ structure.

Up to now, the patterns of the end-bridge structure and paired-di-$\sigma$ structure have not yet been observed and reported in all known STM experiments. As we have demonstrated recently with total energy and reaction pathway calculations, our simulated STM images also clearly show that the di-$\sigma$ structure appears on alternate dimer sites, and the end-bridge structure appears in the paired model.

**3.3. Explanation of STM Images.** In STM imaging, the observed contrast is derived basically from (a) the electronic structure, particularly, the local density of states (LDOSs), close to the $E_F$; (b) the accessibility of the tip to the LDOSs for electron tunneling, including the tip location and bias condition; and (c) the validity of the "featureless" assumption of the wave function of the tip. To investigate the origin of the pattern appearing in the images, such as those in Figures 2 and 5−7, we have calculated and analyzed the surface electronic structures. For example, for the bare Ge(001)c(4 × 2) surface without adsorption, Figure 3a,b shows the side and top views of the charge density plots for the occupied surface states within 0.1 eV below the $E_F$. Such spatial localization of charge is the characteristic of the back-bond states in the energy gap region, and these back-bond states are the main LDOSs giving the contrast in the simulated STM image with $V_S = -0.1$ eV, as shown in Figure 2b. Our calculation results are consistent with the previous results combining STM experiments and first-principles computations[34] and the other results combining photoemission and STM experiments[35] for the electronic structure of Ge(001). In both of these two previous cases, the top valence band of Ge(001) is dominated by the back-bond states. Moreover, the side and top views of charge density plots for the occupied surface states within 0.5 eV below the $E_F$, as shown in Figure 9a,b, indicate that, in addition to the back-bond states, the dangling bond states of the up-Ge atoms can also be observed. Both of them should contribute to the contrast of the stimulated STM image with $V_S = -0.5$ V, as shown in Figure 2a. However, in Figure 9a,b, we can see that the contribution of the dangling bond states is much larger than the contribution of the back-bond states. As such, the simulated STM image in Figure 2a is dominated by the bright protrusions centered on the up-Ge atom, features that reflect the dangling bond states.

For the di-$\sigma$ structure, the partial charge distribution for the occupied states within 0.5 eV below the Fermi level is shown in Figure 9c,d. The spatial localization of charge displays the characteristic of the back-bond and dangling bond states on the unabsorbed Ge dimers, as the charge contribution from the $C_2H_4$ molecule is negligible because the maximum isosurface value of $C_2H_4$ is less than $^1/_{10}$ of the isosuface value of the bare Ge atoms. However, the simulated STM image in Figure 5a only shows patterns of the C atoms of $C_2H_4$ and dangling bonds; the back bonds of Ge atoms are not imaged. Although the charge contribution from $C_2H_4$ is much smaller than the contribution of the dangling bond states under a low bias voltage, the features of the electronic structures from the $C_2H_4$ molecule are the main feature in the simulated STM image. Clearly, this contrast preference for the $C_2H_4$ molecule is related to the relative accessibility of the tip to the LDOSs of the constituents of the probed surface. To clarify the exact contributions from the electronic states of the adsorbed molecules and the bare up-Ge atoms to an STM image at a given bias voltage, we plot the line profiles of the partial charge density versus distance from the Ge(001) surface. Because the contribution of the back-bond states is smaller than the contribution of the dangling bond states, as we have demonstrated for the bare Ge(001)c(4 × 2) surface at a bias of −0.5 V, the line profiles represent that the back-bond states are omitted.

The $z$-line profile of the di-$\sigma$ structure with $V_S = -0.5$ V shown in Figure 10a shows that the maximum line value of the partial charge density around the up-Ge atom is the largest. However, when the STM tip is above the top H atom of the $C_2H_4$ molecule, Figure 10a indicates that the main STM feature will actually be the C2 atom of the $C_2H_4$ molecule (C2 is defined in Figure 5a), with the up-Ge atom as a minor feature. These features are indeed seen in the simulated STM image with $V_S = -0.5$ V, as shown in Figure 5a. As shown in Figure 10b, among the line profiles with $V_S = -1.0$ V, the maximum line value through the up-Ge atom is still the largest one. However, when the STM tip is set above the top H atoms of the $C_2H_4$ molecule for STM image scanning, Figure 10b indicates that the composite of both the two C atoms of the $C_2H_4$ molecule should become the dominant STM feature. In comparison to the data in Figure 10a, the main change from Figure 10a to Figure 10b is the emergence of the C1 atom. A careful comparison of the simulated STM image at $V_S = -1.0$ V (Figure 5b) to that at $V_S = -0.5$ V (Figure 5a) indeed shows some additional STM bright contrast at C1. Finally, when the voltage arrives at −1.5 V, the $z$-line profiles as shown in Figure 10c indicate that the C1 and C2 should become the main STM features, with the up-Ge feature becoming weaker than that in Figures 10b and 5b. Indeed, these changes are seen in the simulated STM image at $V_S = -1.5$ V, as shown in Figure 5c.

The line profiles of the paired-di-$\sigma$ structure are found to be similar to those of the di-$\sigma$ structures. This similarity of the line profiles explains the similarity of the STM images between the di-$\sigma$ structure and paired-di-$\sigma$ structure, as we have mentioned in section 3.2.2.

For the end-bridge structure, Figure 6a shows that the brightness of the spots on the bare up-Ge atoms is different. Hence, we have calculated the line profiles at two up-Ge atoms sites. One is next to the adsorbed dimer, denoted as "site_1″,

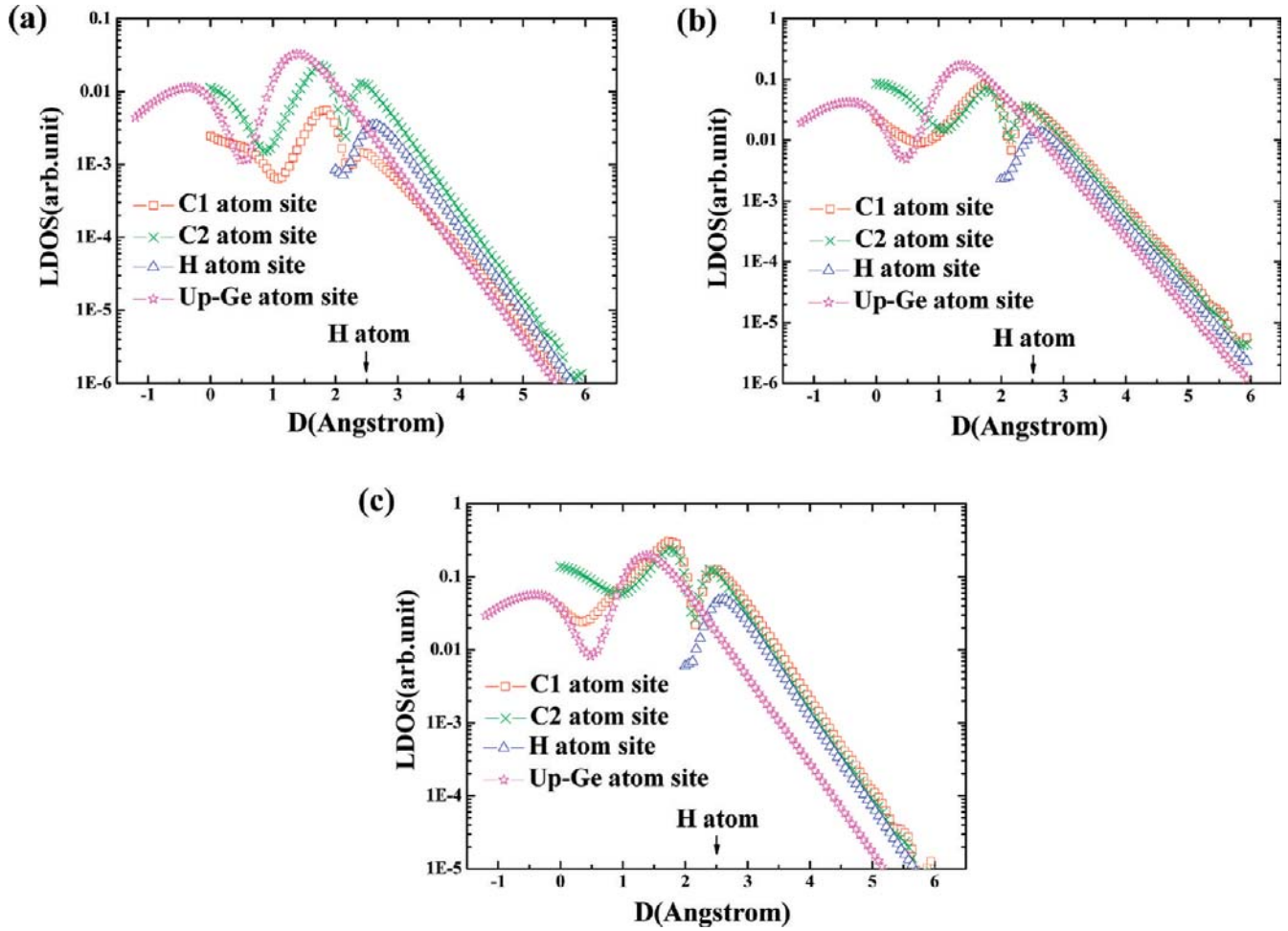


**Figure 10.** Vertical line profiles of the calculated partial charge density versus distance from the Ge(001) surface for the di-$\sigma$ structure with (a) $V_S = -0.5$ V, (b) $V_S = -1.0$ V, and (c) $V_S = -1.5$ V. Four curves representing the partial charge density on the vertical lines through C1, C2, H, and up-Ge atoms are shown. The arrow indicates the height of the top H atom of the $C_2H_4$ on Ge(001).

and the other one is in the other dimer row, denoted as "site_2". Both are shown in Figure 6a. The line profile with $V_S = -0.5$ V is shown in Figure 11a. It shows that the line values through the up-Ge atoms are the largest, and the charge at "site_1" extends further into the vacuum than the charge at "site_2". It is clear that the dominant STM features will be the up-Ge atoms near the adsorbed molecule, whereas those up-Ge atoms further away and the adsorbed molecule are the minor features. This can be found in the STM image shown in Figure 6a. Both of our calculated STM images and line profiles indicate that the end-bridge adsorption does change the near Ge atoms, as we have inferred in our previous report.[20] Figure 11b shows the line profiles with $V_S = -1.0$ V, and the maximum line values through the up-Ge atoms are still the largest ones. In comparison to the data in Figure 11a, the two C atoms of the $C_2H_4$ molecule are emergent, and the difference between the line values at "site_1" and "site_2" is little. Indeed, Figure 6b shows that the brightness of spots on top of all bare up-Ge atoms is almost the same. When the voltage arrives at $-1.5$ V, the $z$-line profiles as shown in Figure 11c indicate that the C and H atoms become the main STM features, whereas the up-Ge feature becomes a little weaker than those of the C and H atoms. These changes can be traced in the careful comparison of the pattern on top of the $C_2H_4$ molecule and up-Ge atom in Figure 6b to those in Figure 6c.

As for the paired-end-bridge structure with two $C_2H_4$ molecules adsorption on the two adjacent dimers, the relative magnitudes of the partial charge of the adsorbed molecules and the unadsorbed up-Ge atoms are similar with the situation of end-bridge adsorption at three bias voltages with $V_S = -0.5$, $-1.0$, and $-1.5$ V. Correspondingly, the similar evolution of the pattern, as shown in Figure 6, for the end-bridge structure on top of the $C_2H_4$ molecule and up-Ge atoms can be found in the images shown in Figure 7 for the paired-end-bridge structure when the bias increases from $-0.5$ to $-1.5$ V.

**3.4. Comparison of STM Images between the Ge(001) and Si(001) Surfaces.** Similar to the Ge(001) surface, the c(4 × 2) surface is also the most stable reconstructed structure for Si(001) surface. The surface states of the Si(001)c(4 × 2) surface near the $E_F$ have been computed to track down the different physical and chemical behaviora recently displayed between the Si and Ge surface. As shown in Figure 12a, the STM image shows the occupied surface states included in 0.2 eV below the $E_F$, which is the occupied dangling bond states centered on the up-Si atoms of the bulk dimers. The partial charge density within 0.2 V below the $E_F$ in Figure 12b,c indicates that the occupied dangling bond states located on the up-Si atoms are the highest occupied surface states. In contrast, the highest occupied surface states on the Ge(001)c(4 × 2) surface are the back-bond states between the top and second layer atoms, as shown in Figure 3. With realizing the difference of the front orbital between the Ge(001) and Si(001) surfaces, one can understand the small adsorption energy and high reaction barrier on the Ge(001) surface relative to those on the Si(001) surface.[9,10] The relevant

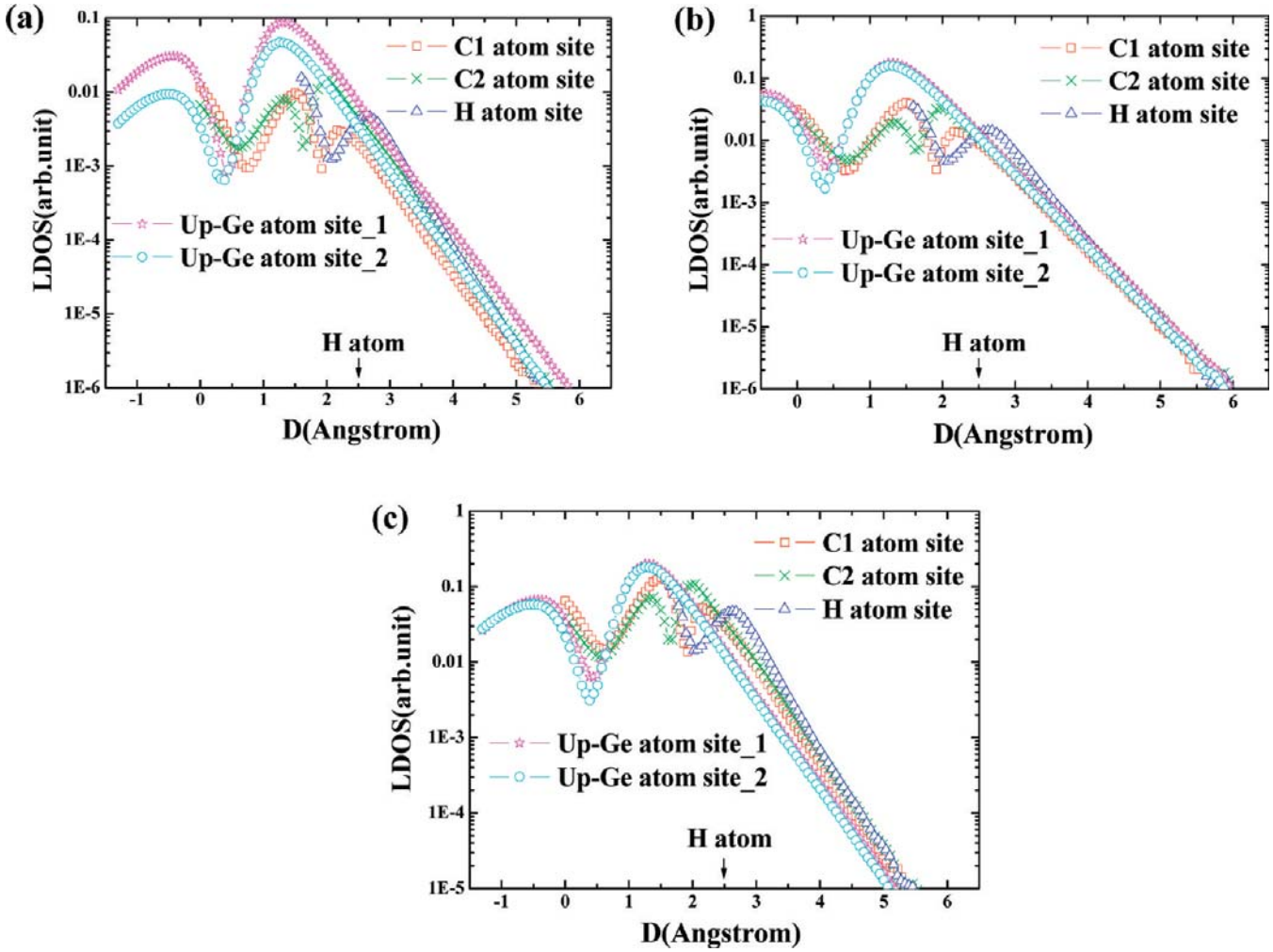


**Figure 11.** Vertical line profiles of calculated partial charge density versus distance from the Ge(001) surface for the paired-end-bridge structure with (a) $V_S = -0.5$ V, (b) $V_S = -1.0$ V, and (c) $V_S = -1.5$ V. Five curves representing the partial charge density on the vertical lines through C1, C2, H, and two up-Ge atoms sites are shown. The arrow indicates the height of the top H atom of the $C_2H_4$ on Ge(001).

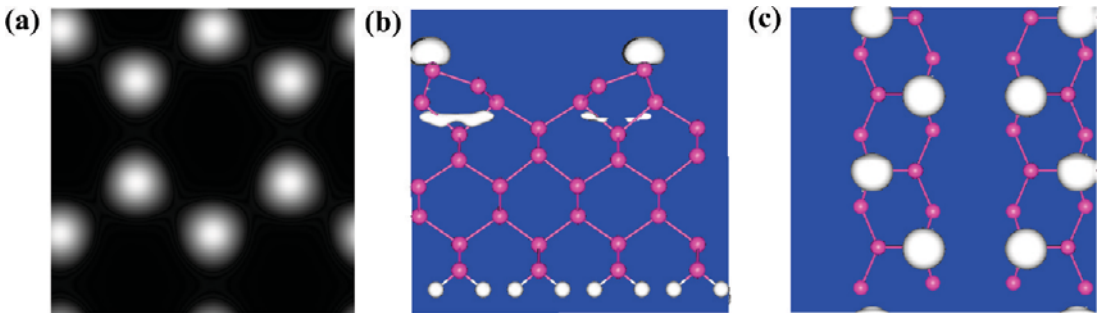


**Figure 12.** (a) Simulated STM image of the bare Si(001)c(4 × 2) surface with $V_S = -0.2$ V. Partial charge density for the bare Si(001)c(4 × 2) surface with $V_S = -0.2$ V: (b) side view and (c) top view.

examples can be found from the adsorption of $C_2H_4$, as listed in Table 1 and the adsorption of $O_2$ molecules in our previous paper.[36]

## 4. Conclusions

Four possible adsorption configurations for $C_2H_4$ on Ge(001) have been considered. Our charge density calculations show that the orbitals of Ge atoms on the surface dominate over the orbital associated with $C_2H_4$ in the region close to the $E_F$. The STM images of these adsorption configurations reflect the feature of the electronic states associated with the adsorbed molecules as well as the electronic states of the Ge atoms because, in the process of STM imaging, the electronic structure and the physical position relative to the tip are the two competing factors. We have demonstrated the topographic effect by the line profile of the partial charge density. Among the four adsorption configurations, only the simulated STM images for the di-$\sigma$ and paired-end-bridge configurations can be compared with the observations in STM experiments. In fact, our simulated STM images and electronic structure calculations prove the two adsorption features observed in STM experiments. Moreover, we display the differences of STM images between Ge(001) and Si(001) and explain the different adsorption behaviors for adsorptions of molecules on Ge(001) in reference to Si(001).

**TABLE 1: Calculated Adsorption Energies, $E_{ads}$(P) and $E_{ads}$(C), and the Reaction Barriers $E_b$ (all in eV) for the Adsorption Structures of $C_2H_4$ on Ge(001) at 0.5 and 1.0 ML. Previous Theoretical Calculations for $C_2H_4$ on Si(001) are Listed[d]**

| | | $C_2H_4$ on Ge(001) | | | $C_2H_4$ on Si(001) | | |
|---|---|---|---|---|---|---|---|
| | | $E_{ads}$(P) | $E_{ads}$(C) | $E_b$ | $E_{ads}$(P) | $E_{ads}$(C) | $E_b$ |
| 0.5 ML | di-$\sigma$ | 0.40 | 1.00 | 0.23 | 0.47[b] | 2.06[a] | 0.07[c] |
| | | | | | 0.48[c] | 1.94[b] | 0.02[b] |
| | end-bridge | 0.35 | 0.90 | 0.19 | 0.45[b] | 1.94[a] | 0.17[c] |
| | | | | | 0.47[c] | 1.82[b] | 0.12[b] |
| 1.0 ML | paired-di-$\sigma$ | 0.23 | 0.97 | 0.17 | 0.31[c] | 1.98[a] | 0.07[c] |
| | | | | | | 1.91[b] | |
| | paired-end-bridge | 0.25 | 1.13 | 0.12 | 0.31[c] | 2.10[a] | 0.07[c] |
| | | | | | | 2.01[b] | |

[a] Reference 17. [b] Reference 18. [c] Reference 19. [d] $E_{ads}$(P) is for the precursor state; $E_{ads}$(C) is for the product chemisorption state.

**Acknowledgment.** The authors thank Professor Zhifeng Liu for valuable discussions. This work was funded by the Discovery Grant program of the Natural Science and Engineering Research Council of Canada (NSERC) for W.M.L., the National Natural Science Foundation of China (NSFC) (20773024) for Y.F.Z., and funds from Shannxi Province (SJ08B14) and the NSFC (20903075) for X.L.F. This work was also supported by the 111 Project (B08040) in China. The authors also acknowledge the support from Surface Science Western and the Faculty of Science at the University of Western Ontario.

## References and Notes

(1) Wolkow, R. A. *Annu. Rev. Phys. Chem.* **1999**, *50*, 413.
(2) Rolfing, M.; Kruger, P.; Pollmann, J. *Phys. Rev. B* **1996**, *54*, 13759.
(3) Zandvielt, H. J. W. *Phys. Rep.* **2003**, *388*, 1.
(4) Gurlu, O.; Zandvliet, H. J. W.; Poelsma, B. *Phys. Rev. Lett.* **2004**, *93*, 066101.
(5) Houselt, A. V.; Gastel, R. V.; Poelsma, B.; Zandvliet, H. J. W. *Phys. Rev. Lett.* **2006**, *97*, 266104.
(6) Loscutoff, P. W.; Bent, S. F. *Annu. Rev. Phys. Chem.* **2006**, *57*, 467.
(7) Cho, Y. E.; Maeng, J. Y.; Kim, S.; Hong, S. *J. Am. Chem. Soc.* **2003**, *125*, 7514.
(8) Filler, M. A.; Mui, C.; Musgrave, C. B.; Bent, S. F. *J. Am. Chem. Soc.* **2003**, *125*, 4928.
(9) Hwang, Y. J.; Hwang, E.; Kim, D. H.; Kim, A.; Hong, S.; Kim, S. *J. Phys. Chem. C* **2009**, *113*, 1426.
(10) Cho, J. H.; Morikawa, E. *J. Chem. Phys.* **2006**, *124*, 024716.
(11) Kim, D. H.; Choi, D. S.; Hong, S.; Kim, S. *J. Phys. Chem. C* **2008**, *112*, 7412.
(12) Shimomura, M.; Munakata, M.; Iwasaki, A.; Ikeda, M.; Abukawa, T.; Sato, K.; Kawawa, T.; Shimizu, H.; Nagashima, N.; Kono, S. *Surf. Sci.* **2002**, *504*, 19.
(13) Matsui, F.; Yeom, H. W.; Matsuda, I.; Ohta, T. *Phys. Rev. B* **2000**, *62*, 5036.
(14) Hennies, F.; Fohlisch, A.; Wurth, W.; Witkowski, N.; Nagasono, M.; Piancastelli, M. N. *Surf. Sci.* **2003**, *529*, 144.
(15) Widdra, W.; Fink, A.; Gokhale, S.; Trischberger, P.; Menzel, D.; Birkenheuer, U.; Gutdeutsch, U.; Rösch, N. *Phys. Rev. Lett.* **1998**, *80*, 4269.
(16) Xu, S. H.; Keeffe, M.; Yang, Y.; Chen, C.; Yu, M.; Lapeyre, G. J.; Rotenberg, E.; Denlinger, J.; Yates, J. T. *Phys. Rev. Lett.* **2000**, *84*, 939.
(17) Marsili, M.; Witkowski, N.; Pulci, O.; Pluchery, O.; Silverstreli, P. L.; Sole, R. D.; Borensztein, Y. *Phys. Rev. B* **2008**, *77*, 125337.
(18) Cho, J. H.; Kleinman, L. *Phys. Rev. B* **2004**, *69*, 075303.
(19) Zhang, Q. J.; Fan, X. L.; Lau, W. M.; Liu, Z. F. *Phys. Rev. B* **2009**, *79*, 195303.
(20) Fan, X. L.; Sun, C. C.; Zhang, Y. F.; Lau, W. M. *J. Phys. Chem. C* **2010**, *114*, 2200.
(21) Lal, P.; Teplyakov, A. V.; Noah, Y.; Kong, M. J.; Wang, G. T.; Bent, S. F. *J. Chem. Phys.* **1999**, *110*, 10545.
(22) Fink, A.; Huber, R.; Widdra, W. *J. Chem. Phys.* **2001**, *115*, 2768.
(23) Kim, A.; Choi, D. S.; Lee, J. Y.; Kim, S. *J. Phys. Chem. B* **2004**, *118*, 3256.
(24) Miotto, R.; Ferraz, A. C.; Srivastava, G. P. *Surf. Sci.* **2002**, *12*, 507.
(25) Tersoff, T.; Hamann, D. R. *Phys. Rev. B* **1985**, *31*, 805.
(26) Kresse, G.; Hafner, J. *Phys. Rev. B* **1993**, *47*, R558.
(27) Kresse, G.; Hafner, J. *Phys. Rev. B* **1994**, *49*, 14251.
(28) Kresse, G.; Furthmüller, J. *Phys. Rev. B* **1996**, *54*, 11169.
(29) Kresse, G.; Furthmüller, J. *Comput. Mater. Sci.* **1996**, *6*, 15.
(30) Vanderbilt, D. *Phys. Rev. B* **1990**, *41*, 7892.
(31) Kresse, G.; Hafner, J. *J. Phys.: Condens. Matter* **1994**, *6*, 8245.
(32) Kresse, G.; Hafner, J. *Phys. Rev. B* **1993**, *48*, 13115.
(33) Perdew, J. P. In *Electronic Structure of Solids '91*; Ziesche, P., Eschrig, H., Eds.; Academie Verlag: Berlin, 1991; p 11.
(34) Radny, M. W.; Schofiled, G. A.; Smith, P. V.; Curson, N. J. *Phys. Rev. Lett.* **2008**, *100*, 246807.
(35) Nakatsuji, K.; Takagi, Y.; Komori, F.; Kusuhara, H.; Ishii, A. *Phys. Rev. B* **2005**, *72*, 241308.
(36) Fan, X. L.; Lau, W. M.; Liu, Z. F. *J. Phys. Chem. C* **2009**, *113*, 8786.

JP101275J